Coseismic displacement waveforms for the 2016 August 24 M_w 6.0 Amatrice earthquake (central Italy) carried out from High-Rate GPS data

A. AVALLONE[1,*], D. LATORRE[1], E. SERPELLONI[1], A. CAVALIERE[2], A. HERRERO[3], G. CECERE[1], N. D'AGOSTINO[1], C. D'AMBROSIO[1], R. DEVOTI[1], R. GIULIANI[4], M. MATTONE[4], S. CALCATERRA[5], P. GAMBINO[5], L. ABRUZZESE[1], V. CARDINALE[1], A. CASTAGNOZZI[1], G. DE LUCA[1], L. FALCO[1], A. MASSUCCI[1], A. MEMMOLO[1], F. MIGLIARI[1], F. MINICHIELLO[1], R. MOSCHILLO[1], L. ZARRILLI[1] AND G. SELVAGGI[1].

[1]Istituto Nazionale di Geofisica e Vulcanologia, Centro Nazionale Terremoti
[2]Istituto Nazionale di Geofisica e Vulcanologia, Sezione di Bologna
[3]Istituto Nazionale di Geofisica e Vulcanologia, Sezione di Roma 1
[4]Ufficio Rischio Sismico e Vulcanico, Dipartimento della Protezione Civile, Roma
[5]Ufficio Geofisica, Istituto Superiore per la Protezione e la Ricerca Ambientale, Roma
*antonio.avallone@ingv.it

Abstract

Abstract: We used High-Rate sampling Global Positioning System (HRGPS) data from 52 permanent stations to retrieve the coseismic dynamic displacements related to the 2016 August 24 Mw 6.0 Amatrice earthquake. The HRGPS position time series (named hereinafter "GPSgrams") were obtained with two different analysis strategies of the raw GPS measurements (Precise Point Positioning [PPP] and Double-Difference [DD] positioning approaches using the Gipsy-Oasis II and the TRACK (GAMIT/GLOBK) software, respectively). These GPSgrams show RMS accuracies mostly within 0.3 cm and, for each site, an agreement within 0.5 cm between the two solutions. By using cross-correlation technique, the GPSgrams are also compared to the doubly-integrated strong motion data at sites where the different instrumentations are co-located in order to recognize in the GPSgrams the seismic waves movements. The high values (mostly greater than 0.6) of the cross-correlation functions between these differently-generated waveforms (GPSgrams and the SM displacement time-histories) at the co-located sites confirm the ability of GPS in providing reliable waveforms for seismological applications.

I. INTRODUCTION

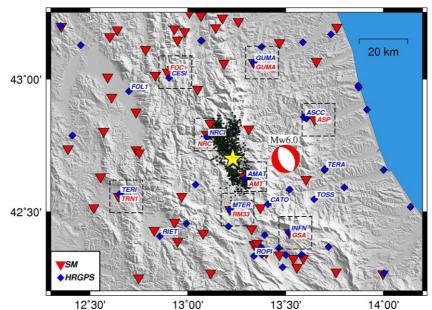On August 24, 2016, at 01:36:32 (UTC time, http://cnt.rm.ingv.it, Marchetti et al., 2016), a M_w 6.0 earthquake struck the region of the Central Apennines (Italy) between the towns of Norcia and Amatrice (Figure 1), where peak ground accelerations values up to 0.9g were recorded (http://ran.protezionecivile.it/). The main

1

shock triggered an aftershock sequence that involved a crustal volume extending SE-NW for ~30 km and down to ~15 km of depth. The main shock and the largest part of aftershock events show focal solutions (http://cnt.rm.ingv.it/tdmt.html, Scognamiglio et al., 2016; http://www.bo.ingv.it/RCMT) characterized by almost pure extension on NW-SE fault planes, in agreement with geodetic measurements of the main event (INGV CNT GPS Working Group, 2016; Cheloni et al., 2016) and with the interseismic SW-NE extension characterizing this sector of the Apennines (e.g., Galvani et al., 2012; D'Agostino, 2014).

The ground displacements associated to the August, 24 M_w 6.0 main shock were recorded by a number of High-Rate sampling (from 1 to 0.05 s) continuous GPS (HRGPS) stations (Figure 1) belonging to several networks developed for both scientific and surveying purposes. In detail, raw phase data were obtained from the following GNSS networks or agencies: RING (INGV RING Working Group, 2016; http://ring.gm.ingv.it), ISPRA (http://www.isprambiente.gov.it), DPC (http://www.protezionecivile.gov.it), Regione Lazio (http://gnss-regionelazio.dyndns.org), Regione Abruzzo (http://gnssnet.regione.abruzzo.it), ITALPOS (http://it.smartnet-eu.com) and NETGEO (http://www.netgeo.it). The main shock was also recorded by several strong motion (SM) stations belonging to the INGV Rete Sismica Nazionale (RSN, INGV Seismological Data Centre, 1997) and the DPC Rete Accelerometica Nazionale (RAN, http://ran.protezionecivile.it) accelerometric networks.

This work is within the line of GPS seismology (Larson et al., 2003; Bock et al., 2004, Larson et al., 2009), in which the estimation of the coseismic dynamic displacements is carried out following different methods (i.e. Precise Point Positioning [PPP, Zumberge et al., 1997; Bertiger et al., 2010], Double-Difference (DD) Positioning [Herring et al., 2010]), variometric [Colosimo et al., 2011] and ambiguity constrained time-differences [Li et al., 2013] approaches). In this work we will describe the high-rate GPS (HRGPS) time series (named hereinafter "GPSgrams") following the PPP and DD approaches by using two different scientific packages (Gipsy/Oasis and GAMIT/GLOBK), and compare the results. The GPSgrams have been also compared with the displacement time histories carried out from the double integration of the SM data at some stations, where the different instruments are approximately co-located (Figure 1).

II. HRGPS TIME SERIES

The available HRGPS data were analyzed with two different approaches (PPP and DD strategies), using two non-commercial, geodetic-quality, software modules for kinematic processing: the TRACK module of GAMIT/GLOBK developed at the Massachusetts Institute of Technology (http://wwwgpsg.mit.edu/~simon/gtgk/, Herring et al., 2010), and the GD2P module of GIPSY/OASIS II, developed at the Jet Propulsion Laboratory (http://gipsy.jpl.nasa.gov, Bertiger et al., 2010). For the description of the detailed aspects related to the analysis strategies we refer to Avallone et al. (2012). For the general description of the detailed aspects related to the analysis strategies we refer to Avallone et al. (2012). However, with respect to this previous work, during the analysis we applied improved available models of the troposphere (Bohem et al. 2006) and second order ionosphere (Kedar et al., 2003) estimations

2

Figure 1: *Locations of the HRGPS stations (blue diamonds) and of the SM stations (red triangles) operating during the Amatrice 2016 main shock. The star represents the location of the main shock, whereas the green dots show the distribution of the aftershocks occurred within the first two days from the main shock (http://cnt.rm.ingv.it, Marchetti et al., 2016). The focal mechanism (Scognamiglio et al., 2016; http://cnt.rm.ingv.it/tdmt.html) is normal. The GPSgrams of the labeled HRGPS sites are shown in Figure 2A-B, whereas the open squares indicate the couples of HRGPS and SM sites used for the comparisons in Figure 3.*
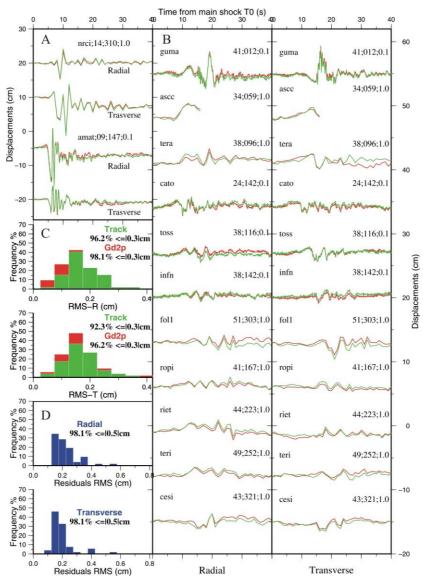
(VMF1 grid and IONEX files, respectively). It is worth noting that the two software packages are based on a completely different approach in the reduction of the raw phase data: the GD2P module follows the PPP approach, where the kinematic station only needs fiducial high-rate satellite orbits and clocks information; the TRACK module performs relative kinematic positioning and it needs at least one reference station out of the epicentral area (i.e., assumed fixed in the time interval affected by the dynamic displacements in the epicentral area), and one (or more) kinematic station. In this study, after an analysis of the quality of the satellite tracking at different potential reference (fixed) stations (i.e. sky plots, multipath and cycle-slips metrics) and of the resolved parameters (i.e. ambiguity fixing), the station

CASS (Cassino, Lat: 41.49; Lon: 13.83, ~140 km from the epicenter), belonging to the Regione Lazio GNSS network, was chosen as the reference site for the analysis with TRACK of all the stations located within 50 km from the epicenter. The relative double-difference positioning performed in the TRACK analysis likely allows to remove, or at least minimize, a common-mode regional contribution that could be, on the contrary, present, as low-frequency contribution, in the PPP solutions. For this reason, we applied to the GD2P solutions a spatial filtering commonly used for filtering long-term (daily positions) time series (Wdowinski et al., 1997). In detail, we firstly selected the GPSgrams not affected by coseismic dynamic displacements in the time interval 0-40s. These GPSgrams, corresponding to the 9 sites be-

3

longing to the Regione Lazio GNSS network located outside the epicentral area (more than 50 km from the epicenter), were then stacked and averaged. Finally, we removed this averaged signal from the GPSgrams located in the epicentral area.

By using the SAC software (Goldstein et al., 2005), distributed by IRIS (Incorporated Research Institutions for Seismology), the North and East components of the measured ground displacements at each site were rotated with respect to the epicenter and presented in the Radial-Transverse coordinate system, since the radial (R) component mainly contains SV and P-wave arrivals, while the transverse (T) component presents predominantly SH-wave modes. This representation may be not optimal in near source regions as in the case of NRCI and AMAT stations (Figure 1). Nevertheless, in this particular case, we can adopt the RT representations because both the stations are located along the strike of the M6 event and the RT components correspond to the fault-parallel and fault-normal components, respectively.

In Figure 2, some examples of comparison on both radial and transverse components as obtained by the two different solutions are shown for the sites labeled in Figure 1, whereas the comparison between both the solutions for all the 52 sites are shown in Figure SM1 of the Supplementary Material. A first comparison is focused on the two GPS sites located closer to the epicenter (AMAT, Amatrice, ~9 km to the SE, and NRCI, Norcia, ~14 km to the NW, Figure 2A). AMAT acquired data at 0.1 s sampling rates, thus allowing potentially low aliasing artifacts in the observations (Smalley, 2009; Avallone et al., 2011), whereas NRCI acquired data at 1 s sampling rate. Because of their proximity to the epicenter, they experi-

enced the largest coseismic dynamic displacements: AMAT shows larger values of peak-to-peak displacements on the radial component (~16.6 cm) than on the transverse one (~8.2 cm), whereas NRCI shows generally lower peak-to-peak displacements than AMAT, but larger on the transverse component (~15.0 cm) than on the radial one (~8.2 cm). The comparisons between the GD2P and TRACK results are also shown in Figure 2B at some sites located between ~35 and ~50 km from the epicenter, where the static deformation due to the near field is expected to be negligible (as shown in Cheloni et al., 2016) or within the accuracy of the HRGPS time series. The GPSgrams shown from the top to the bottom of the Figure 2B are sorted by increasing azimuth angle and seem to point out the SH arrivals on the T component and the surface waves arrivals on the R component in the time ranges 10-15 s and 15-25 s, respectively.

Due to power failures occurred a few seconds after the main shock, likely related to the S-wave arrivals ground motion, the available data and the resulting GPSgrams at some sites (LNSS, ASCC, ASCO and CAMR) are suddenly truncated. One of these examples (ASCC) is shown in Figure 2B.

The comparison between GD2P and TRACK solutions (in both the Figure 2B and the Figure SM1) shows a remarkable agreement in the detection of the higher-frequency coseismic dynamic displacements, observing comparable peak-to-peak values. To quantify the noise level of our GPSgrams, for all the sites we calculated the RMS of the position time series in a 10-s time window before the earthquake origin time. In Figure 2C, the histograms of the RMS distributions of all the available sites are shown for both the R and T components and for the GD2P and TRACK
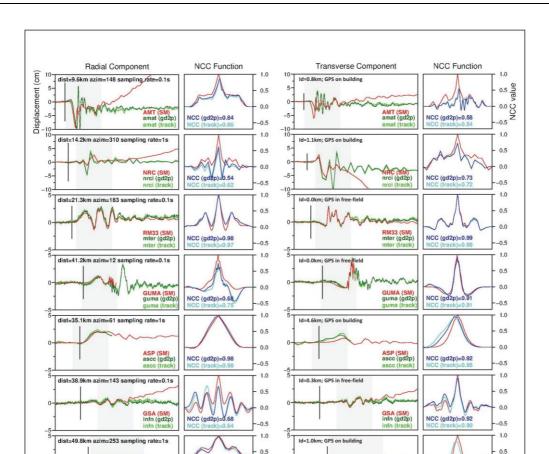
4

Figure 2: *A) Comparison between the GD2P and TRACK GPSgrams for the two stations closest to the epicenter (AMAT, Amatrice, and NRCI, Norcia) on the Radial and Transverse components; B) Radial (left) and Transverse (right) components of the GD2P (red) and TRACK (green) GPSgrams obtained for the sites labeled in Figure 1, between 35 and 50 km from the epicenter in a time interval of 40 s starting from the main shock origin time (01:36:32 UTC, http://cnt.rm.ingv.it). In both the panels, from top to down the sites are sorted by the increasing azimuth degree. Labels and numbers on each time series represent the name of the sites, the azimuth degree, the distance from the epicenter and the sampling rate, respectively; C) RMS histogram distributions calculated in a pre-seismic 10-s time window for GD2P (red) and TRACK (green) on both Radial (top) and Transverse (bottom) components for all the 52 solutions. D) RMS histogram distributions of the differences between the GD2P and TRACK solutions in a time interval of 0-40 s on both Radial (top) and Transverse (bottom) components for all the 52 solutions.*

solutions. Two features are worth noting: a) 92% to 98% of the GPSgrams reveal values of accuracy within 0.3 cm; b) the radial and transverse components seem to show comparable accuracies' distribution between GD2P and TRACK. Finally, to quantify the consistency between the GD2P and the TRACK solutions, for each site, we firstly calculated the epoch-by-epoch differences between the two solutions and then we estimated the RMS distribution of the so determined residuals. The histograms of the residuals' RMS distribution (Figure 2D) show that for most of the sites, the two solutions agree within a value of 0.5 cm. The results obtained in this work show scatter values in the solutions reduced by about 50% with respect to a similar analysis carried out for the Emilia sequence (Avallone et al., 2012).

III. COMPARISON BETWEEN HRGPS AND STRONG MOTION

In this work we selected 8 examples of SM stations approximately co-located with the HRGPS sites. For most of the sites (six examples), the relative distance between the co-located instrumentations ranges from 0 to 1.1 km. However, we also included the FOC and ASP SM stations whose relative distances with GPS instrumentation (CESI and ASCC, respectively) are higher, about 2.4 and 4.6 km, respectively.

In order to compare HRGPS and accelerometric time series, we transformed in displacement the SM recordings by applying a double-integration after removing the mean of the signal calculated in a 4-s time window before the P-wave first-arrival. Moreover, since SM data were recorded with higher sampling rate (0.005 s) than HRGPS data (1 s and 0.1 s,

Figure 2), we firstly filtered the SM-data at the associated GPSgram Nyquist frequency to avoid any aliasing effect, and then we decimated each SM displacement waveform at the sampling rate of the co-located GPS instrument. To quantify the similarity between the SM displacement waveforms and the GPSgrams, we performed a normalized cross-correlation (NCC) between the signals recorded in a time window of 10 s after the P-wave first arrival. The analysis of source radiation recorded at the co-located SM and GPS stations is shown in Figure 3 in terms of their ground-motion displacement in the RT coordinate system, following the same procedure used to compare the two GPSgrams solutions. As a first approximation, we find a good agreement between the processed GPSgrams and the doubly-integrated SM data. This match can be also deduced from the cross-correlation function computed for windows of signals that include the first coseismic dynamic displacements. Due to the minimum processing applied to the SM data, we observe a strong t^2-drift, shortly after the S-wave arrival, for stations located in near field (AMT, NRC). Such drifts are well known in literature and are the effect of small distortions in acceleration, often due to static displacements, that appear when waveforms are double integrated (e.g., Boore et al., 2002). Other smaller offsets are observed at other stations more distant from the source, but they are difficult to quantify over this time window. The main difference between integrated accelerograms and GPSgrams in terms of peak of displacement is observed for the two stations located near the fault (AMT-AMAT and NRC-NRCI). For the R component of the AMT station, the integrated accelerogram shows only one peak, while the GPS shows a comparable (in amplitude peak), and a second later peak with amplitude similar

Figure 3: *Examples of comparison between GPSgrams (GD2P and TRACK solutions, dark and light green lines, respectively) and the SM displacement time-series (red lines) at 8 co-located sites. Data are presented along the Radial (1st column) and the Transverse (3rd column) component. In 2nd and 4th columns are also plotted the normalized autocorrelation function (ACC, red line) and the normalized cross-correlation (NCC) functions between GD2P and SM time-series (dark blue), and between TRACK and SM time-series (light blue) computed for both R and T components. The maximum NCC value for each GPS-SM time series is reported in the figure. ACC and NCCs were computed between signals recorded in windows of 10 s (gray area), 1-2 seconds after the P-wave first arrival time, picked on the strong motion waveform in acceleration and indicated with a vertical black bar. Only for signals at GUMA and ASP stations the window is smaller (9 seconds) due to the interruption of the SM recording in the first case and of the GPS acquisition in the second one. The text in the figures explicit the distance (dist) and the azimuth (azim) with respect to the epicenter, the sampling rates, the inter-distance (Id) between the SM and the GPS and, finally, the type of installation of the GPS antenna (building or free-field).*

to the first one. GPS and SM displacements are similar for the first peak on the T component whereas the following portions of the signals present significant differences with higher GPS amplitudes. These differences cannot be explained with eventual inaccuracy of the processing because these kinds of frequencies are very well reproduced on GUMA station for instance. Since the GPS antennas at NRCI and AMAT sites were installed on the top of buildings, possible amplifications related to the response of the building to coseismic shaking should be more carefully evaluated, considering both its structure and orientation. However, due to the similarity of the first seconds after the P-first arrival, we find that the NCC value for AMAT is still very high on the R component (0.84-0.86). Similar characteristics are observed for NRCI that shows a high NCC value on the T component (0.72-0.73). Here, the differences in amplitude are mainly due to the down-sampling of the SM data at 1 s, while we find that the PGD (Peak Ground Displacement) on the T component is not driven by the same peak possibly due to site effects.

RM33-MTER co-located stations are the first that present very coherent signals on both the components. The double-integrated SM signal and the GD2P and TRAK solutions show maximum NCC values of 0.98 and 0.97 on the R and T components, respectively, indicating that the GPS is able to perfectly reproduce the coseismic dynamic displacements. In this case, the MTER station has the advantage to be installed in free-field, avoiding possible problems of amplifications related to the installation.

The global pattern of PGD on four co-located stations ASP-ASCC, GSA-INFN, TRN1-TERI and FOC-CESI is compatible with the focal mechanism of the M6 event. Indeed, these set of stations are located along the nodal planes that reduce the amplitude of the SH-wave, generally identified along the T-component. The agreement between GPS and integrated SM signals is globally good, even for stations as ASP-ASCC and FOC-CESI that are not perfectly co-located (inter-distance of 2.4 km and 4.6 km, respectively, Figure 1). This is visible on the cross-correlation functions that have high maximum values, but are shifted in time with respect to the autocorrelation function computed on the SM signal.

The amplitudes recorded at the GUMA station are compatible with a directivity toward the Nord. This is evident by comparing the amplitudes recorded at the other stations, including RM33 that is closer to the epicentral area (Figure 1). At GUMA station, the accelerometer recording stopped just after the peak over the T-component. After that, a greater peak is observed on the R-component of the GPSgrams. This signal corresponds to a Rayleigh-type surface wave since a similar peak is also identified on the Z-component with the typical dephasing of $\pi/2$. The same kind of wave is also observed on the co-located FOC-CESI stations, demonstrating that the PGD is rapidly associated to the surface wave when the epicentral distance increases.

IV. CONCLUSIONS

The analysis of high-rate coseismic dynamic displacements of the 2016 August 24 M_w 6.0 Amatrice earthquake were carried out at 52 continuous GPS stations. The observed ground motions in the GPSgrams were consistently associated with the propagation of the seismic waves. As expected, the HRGPS ability to detect details in the seismic waves increases with the increasing of the sampling frequency of the acquired raw data. Furthermore, acquiring data with high sampling frequencies (> 5 Hz) not

only strongly reduce aliasing artifacts in the resulting GPSgrams near the source (Smalley, 2009; Avallone et al., 2011), but it also allows to observe details in the seismic wave propagation in the far field. For this earthquake, in fact, appreciable differences in the observations of the surface waves arrivals still exist between the 10-Hz-sampling (i.e., GUMA) and the 1-Hz-sampling (i.e., CESI) GPSgrams even at larger distances from the epicenter (35-50 km).

For the moderate earthquakes occurred in Italy in the last 8 years (2009 M_w 6.3 L'Aquila; 2012 M_w 5.9 and M_w 5.8 Emilia main shocks, 2016 M_w 6.0 Amatrice) we observe a relatively good spatial coverage of the HRGPS stations around the epicenter, although the contribute of non-geophysical GNSS networks in this picture is still significant. Further efforts in developing denser HRGPS networks, with efficient coupling of the antenna installations with the solid Earth, and operating at sampling frequencies ≥ 10 Hz would provide additional constraints to characterize the source process and discriminate peculiar site effects (Avallone et al., 2014).

With respect to the case of the 2012 Emilia earthquake (Avallone et al., 2012), the observed GPSgrams for different software packages show a factor-2 lower RMS values (0.3 cm) and residuals RMS values (0.5 cm) suggesting a very good accuracy and agreement in the observation of the coseismic dynamic displacements. In addition, the high values of the cross-correlation functions between the GPSgrams and the SM displacement time-histories at the co-located sites confirm the ability of GPS in providing reliable waveforms for seismological applications.

The GPSgrams described in this work represent a potential contribution to further studies on the earthquake source. Significant improvements of (1) the source rupture kinematic modeling, in (2) definition of source directivity generated by the main shock, or (3) for estimating the magnitude of the event could be obtained by the joint use of GPSgrams and strong motion waveforms. In fact, in seismology and engineering seismology, the estimation of the PGD is useful for studies on earthquake processes, seismic design and structural monitoring (i.e. building, bridges). However, using conventional seismological approaches this estimation is still challenging. On the other hand, positions correspond to basic observations for the GPS. In this sense, the GPSgrams could today provide important and decisive contributions to investigate earthquake radiation pattern and source directivity estimating the PGD distribution around the seismic source.

REFERENCES

Avallone *et al.* (2011), Very high rate (10 Hz) GPS seismology for moderate-magnitude earthquakes: The case of the Mw 6.3 L'Aquila (central Italy) event, *J. Geophys. Res.*, 116, B02305, doi: 10.1029/2010JB007834.

Avallone, A. *et al.* (2012). High-rate (1 Hz to 20-Hz) GPS co-seismic dynamic displacements carried out during the Emilia 2012 seismic sequence, *Ann. Geophys.*, 55 (4); doi:10.4401/ag-6162.

Avallone, A. *et al.* (2014), Waveguide effects in very high rate GPS record of the 6 April 2009, Mw 6.1 L'Aquila, central Italy earthquake, *J. Geophys. Res. Solid Earth*, 119, 490–501, doi: 10.1002/2013JB010475.

Bertiger, W., S. Desai, B. Haines, N. Harvey, A. Moore, S. Owen, J. Weiss (2010), Single receiver phase ambiguity resolution with GPS data, *J. Geod.*, 84, 5 (May 2010), pp. 327-337.

Bock, Y., L. Prawirodirdjo, and T. I. Melbourne (2004), Detection of arbitrarily large dy-

namic ground motions with a dense high-rate GPS network, *Geophys. Res. Lett.*, 31, L06604, doi:10.1029/2003GL019150.

Boehm, J. Werl, B. & Schuh, H. (2006), Troposphere mapping functions for GPS and very long baseline interferometry from European Centre for Medium-Range Weather Forecasts operational analysis data. *J. Geophys. Res.*, 111, B02406, doi: 10.1029/2005JB003629.

Boore, D. M., C. D. Stephens and W. B. Joyner (2002), Comments on Baseline Correction of Digital Strong-Motion Data: Examples from the 1999 Hector Mine, California, Earthquake, *Bull. Seism. Soc. Am.*, 92, 4, 1543-1560, doi: 10.1785/0120000926.

Cheloni, D. *et al.* (2016), GPS observations of coseismic deformation following the 2016, August 24, Mw 6 Amatrice earthquake (central Italy): data, analysis and preliminary fault model, *Ann. Geophys.*, 59, FAST TRACK 5, doi:10.4401/ag-7269.

Colosimo, G., M. Crespi, and A. Mazzoni (2011), Real-time GPS seismology with a stand-alone receiver: A preliminary feasibility demonstration, *J. Geophys. Res.*, 116, B11302, doi:10.1029/2010JB007941.

D'Agostino, N. (2014), Complete seismic release of tectonic strain and earthquake recurrence in the Apennines (Italy), *Geophys. Res. Lett.*, 41, 1155–1162, doi: 10.1002/2014GL059230.

Galvani, A. *et al.* (2012). The interseismic velocity field of the central Apennines from a dense GPS network. *Ann. Geophys.*, 55, 5, 2012; doi: 10.4401/ag-5634.

Goldstein, P., D. Dodge, M. Firpo, Lee Minner (2003), "SAC2000: Signal processing and analysis tools for seismologists and engineers", Invited contribution to "The IASPEI International Handbook of Earthquake and Engineering Seismology", Edited by WHK Lee, H. Kanamori, P.C. Jennings, and C. Kisslinger, Academic Press, London.

Herring, T., King, R.W. & McClusky, S., (2010), GAMIT Reference Manual, Release 10.4, Massachussetts Institute of Technology, Cambridge, MA.

INGV-CNT GPS Working Group (2016), Co-seismic displacements for the August 24, 2016 Ml6, Amatrice (central Italy) earthquake estimated from continuous GPS stations, doi:10.5281/zenodo.61355.

INGV RING Working Group (2016), Rete Integrata Nazionale GPS, doi:10.13127/RING.

INGV Seismological Data Centre (1997), Rete Sismica Nazionale (RSN), doi: 10.13127/SD/X0FXNH7QFY

Kedar, S., G. A. Hajj, B. D. Wilson, and M. B. Heflin (2003), The effect of the second order GPS ionospheric correction on receiver positions, *Geophys. Res. Lett.*, 30, 1829, doi:10.1029/2003GL017639, 16.

Larson, K. M., P. Bodin, and J. Gomberg (2003), Using 1-Hz GPS data to measure deformations caused by the Denali fault earthquake, *Science*, 300, 1421–1424, doi: 10.1126/science.1084531.

Li, X. *et al.* (2013), Real-time high-rate coseismic displacement from ambiguity-fixed precise point positioning: Application to earthquake early warning, *Geophys. Res. Lett.*, 40, 295–300, doi:10.1002/grl.50138.

Marchetti et al. (2016). The Italian Seismic Bulletin: strategies, revised pickings and locations of the Amatrice seismic sequence, *Ann. Geophys.*, 59, FAST TRACK 5, doi:10.4401/ag-7169.

Scognamiglio, L., E. Tinti and M. Quintiliani (2016), The first month of the 2016 central Italy seismic sequence: fast determination of time domain moment tensors and finite fault model analysis of the ML 5.4 after-

shock, *Ann. Geophys.*, 59, FAST TRACK 5, doi: 10.4401/ag-7246.

Smalley, R. Jr. (2009), High-rate GPS: How high do we need to go?, *Seism. Res. Lett.*, 80, 1054-1061, doi:10.1785/gssrl.80.6.1054.

Wdowinski, S., Y. *et al.* (1997), Southern California permanent GPS geodetic array: Spatial filtering of daily positions for estimating coseismic and postseismic displacements induced by the 1992 Landers earthquake, *J. Geophys. Res.*, 102(B8), 18057–18070, doi:10.1029/97JB01378.

Wessel, P., and W. H. F. Smith (1998), New, improved version of generic mapping tools released, *Eos Trans. AGU*, 79, 579.

Zumberge, J. F. *et al.* (1997), Precise point positioning for the efficient and robust analysis of GPS data from large networks, *J. Geophys. Res.*, 102(B3), 5005-5018.